THE JOURNAL OF BIOLOGICAL CHEMISTRY VOL. 289, NO. 27, pp. 18614–18624, July 4, 2014

Study of the Protein Complex, Pore Diameter, and Pore-forming Activity of the *Borrelia burgdorferi* P13 Porin*[S]

Received for publication, November 30, 2013, and in revised form, May 10, 2014 Published, JBC Papers in Press, May 13, 2014, DOI 10.1074/jbc.M113.539528

Iván Bárcena-Uribarri[‡§1], Marcus Thein[‡], Mariam Barbot[‡], Eulalia Sans-Serramitjana[‡], Mari Bonde[¶], Reinhard Mentele[‖], Friedrich Lottspeich[‖], Sven Bergström[¶], and Roland Benz[‡§]

From the [‡]Rudolf-Virchow-Center, Deutsche Forschungsgemeinschaft Research Center for Experimental Biomedicine, University of Würzburg, Versbacher Strasse 9, D-97078 Würzburg, Germany, [§]School of Engineering and Science, Jacobs University Bremen, Campusring 1, D-28759 Bremen, Germany, [¶]Department of Molecular Biology, Umeå University, S-90187 Umeå, Sweden, and [‖]Max-Planck Institute of Biochemistry, Protein Analysis Department, Am Klopferspitz 18, D-82152 Martinsried, Germany

Background: *B. burgdorferi* P13 has unique characteristics compared with other porins.
Results: P13 is a homo-oligomer with a 0.6 nS conductance in 1 M KCl and a substrate cut-off of 400 Da.
Conclusion: P13 represents a general diffusion pathway for small solutes into *Borrelia*.
Significance: Understanding the molecular transport through P13 may play a role in designing more efficient antibiotic treatments against *Borrelia* infections.

P13 is one of the major outer membrane proteins of *Borrelia burgdorferi*. Previous studies described P13 as a porin. In the present study some structure and function aspects of P13 were studied. P13 showed according to lipid bilayer studies a channel-forming activity of 0.6 nanosiemens in 1 M KCl. Single channel and selectivity measurements demonstrated that P13 had no preference for either cations or anions and showed no voltage-gating up to ±100 mV. Blue native polyacrylamide gel electrophoresis was used to isolate and characterize the P13 protein complex in its native state. The complex had a high molecular mass of about 300 kDa and was only composed of P13 monomers. The channel size was investigated using non-electrolytes revealing an apparent diameter of about 1.4 nm with a 400-Da molecular mass cut-off. Multichannel titrations with different substrates reinforced the idea that P13 forms a general diffusion channel. The identity of P13 within the complex was confirmed by second dimension SDS-PAGE, Western blotting, mass spectrometry, and the use of a *p13* deletion mutant strain. The results suggested that P13 is the protein responsible for the 0.6-nanosiemens pore-forming activity in the outer membrane of *B. burgdorferi*.

The genus *Borrelia* belongs to the Spirochetes phylum, which is distantly related to Gram-negative bacteria (1). *Borrelia* sp. are pathogenic bacteria that can cause two diseases, Lyme disease and relapsing fever (2–4). *Borrelia burgdorferi*, the most well studied species in this genus, is one of the causative agents of the Lyme disease, a multisystemic disease that can affect different organs during infection, such as skin, joints, and nervous system (5, 6).

Borrelia species are found associated with various hosts, which is attributed to their limited metabolic capacity (7). *Borrelia* sp. lack genes involved in the biosynthesis of amino acids, fatty acids, and nucleotides pointing to the need of getting additional nutrients from their different hosts (8). These molecules must be taken up from the vertebrate hosts including birds or the invertebrate tick vector (9, 10). The first step in nutrient uptake in Gram-negative bacteria is accomplished by porins. Bacterial porins are water-filled channels that facilitate the transport of essential molecules across the outer membrane (11). Most of the porins found in the outer membranes of Gram-negative bacteria are composed of antiparallel β-sheets forming β-barrel cylinders. Frequently, they are arranged as oligomers, usually trimers, which provide a high stability to the protein complex (11, 12). Porins can be classified in two groups depending on their function; as general diffusion porins when they sort simply according to the molecular mass of the solutes or as substrate-specific porins when facilitating the transport of classes of molecules such as carbohydrates, nucleotides, or phosphate (11, 13–17).

Three porins have previously been described in *Borrelia* sp. P66 and P13 were found in Lyme disease *B. burgdorferi*, whereas Oms38 was first discovered in relapsing fever spirochetes. Subsequently, an Oms38 homologue, called DipA, has been found in *B. burgdorferi*. P66 has a remarkably high single channel conductance, and it is the best studied pore-forming protein in *Borrelia* sp. (18–21). Oms38/DipA has been identified to be a porin-specific for dicarboxylates (22, 23).

P13, the subject of this study, represents an atypical type of porin. It forms channels in the outer membrane of *Borrelia* despite its small 13-kDa molecular mass and its α-helical secondary structure (24). The occurrence and function of a

* This work was supported by a joint project between Stint (Sweden) and Deutscher Akademischer Austauschdienst (DAAD) (Germany) (to S. B. and R. B.), the Deutsche Forschungsgemeinschaft (Be 864/15-1; to R. B.), Wi 933 (to Mathias Winterhalter), and Swedish Medical Research Council Grant 07922 (to S. B.).
[S] This article contains supplemental Fig. S1–S4.
[1] Supported by the Alfonso Martín Escudero Foundation. To whom correspondence should be addressed: School of Engineering and Science, Jacobs University Bremen, Campusring 1, D-28759 Bremen, Germany. Tel.: 49-421-200-3583; Fax: 49-421-200-3249; E-mail: i.barcenauribarri@jacobs-university.de.

periplasmic peptide derived from cleavage of its C-terminal end is not completely understood and is unique among porins (25, 26). Another very remarkable feature of P13 is the presence of up to eight paralogues in the genome of *B. burgdorferi* (27). The only paralogue further studied is BBA01, also showing pore forming activity (28). The reason for the high copy number of genes coding for P13-like proteins is still not understood, but it reinforces the idea that P13 could be an indispensable outer membrane protein.

Another protein called Oms28, which is exported to the periplasm, was initially described as a porin with a 0.6-nanosiemen (nS)[2] single channel conductance (29). Afterward, its function as a porin was questioned due to its periplasmic membrane-associated location (30, 31).

In the present study structure and composition of the P13 protein complex was studied with blue native PAGE (BN-PAGE). Furthermore, the biophysical properties of the complex were investigated. In particular, we studied its single channel activity in different salt solutions, ion selectivity, voltage-gating, and the possibility of substrate specificity. Similarly, the diameter of the P13 channel was evaluated using different non-electrolytes. Surprisingly, the 0.6-nS single channel conductance of P13 described in this study was completely different to the 3.5-nS conductance previously reported (24).

EXPERIMENTAL PROCEDURES

Bacterial Strains and Isolation of the Outer Membrane Proteome

B. burgdorferi B31 (ATCC35210) high passage, and *B. burgdorferi* P13–18 (32) were cultivated in BSKII medium as previously described (33). The isolation of outer membrane proteins (B-Fraction) was performed following a previously published protocol (34).

Study of the P13 Complex by Blue Native PAGE and SDS-PAGE

BN-PAGE in First Dimension—Approximately 1.8 μg of B-fraction was solubilized in 25 μl of 10 mM digitonin by incubation for 15 min at room temperature. After solubilization the sample was centrifuged at 20,000 $\times$ *g* for 20 min at 4 °C. The remaining unsolubilized proteins in the pellet were discarded. The supernatant was mixed 5:1 v/v with 50% glycerol and then 15:1 v/v with 5% Coomassie G-250 right before loading the BN-PAGE.

NativePAGE™ Novex® 4–16% Bis-Tris gels 1.0 mm (Invitrogen) were used. The conditions recommended by the manufacturers were used for electrophoresis (150 V constant). One-third of the run was performed in the presence of deep blue cathode buffer, and the remaining two-thirds were run using light blue cathode buffer. The corresponding P13 band was eluted from the gel and run again on a BN-PAGE to eliminate the remaining proteins from the membrane extract that tended to smear on the first BN-PAGE. To extract the P13 complex, the corresponding band was excised with a clean scalpel. The gel was crushed into pieces and mixed 1:2 w/v with 0.1% digitonin. The mixture was incubated overnight in a shaker at 4 °C. For reloading the sample on another BN-PAGE, the protein solution was mixed 5:1 v/v with 50% glycerol and then 30:1 v/v with 5% Coomassie solution before the sample was loaded on the gel. The conditions for electrophoresis remained the same as for the first BN-PAGE.

Tricine SDS-PAGE—The P13 complex eluted from a native gel was resolved in Tricine gels (Novex® 16% Tricine gels 1.0 mm, Invitrogen) after mixing with SDS sample buffer and heating the sample for 10 min at 95 °C. The gels were run using MES SDS running buffer following the instructions of the manufacturer.

SDS-PAGE in Second Dimension—Second dimension SDS-PAGE (NuPAGE® Novex 12% Bis-Tris gel 1.0-mm 2D Well, Invitrogen) was used to dissect the P13 complex after BN-PAGE. A lane of the BN-PAGE was cut and incubated in three denaturing solutions according to manufacturer's instructions (Invitrogen). The lane of the gel was incubated for 30 min in the reducing and alkylating solutions and then 15 min in the quenching solution. Electrophoresis was performed as recommended by the manufacturer (Invitrogen) using MES SDS running buffer. BN- and SDS-PAGE were stained with silver nitrate following protocols described elsewhere (35, 36).

Western Blots (WB)—BN- and SDS-PAGE were blotted onto 0.2-μm pore size PVDF membranes (Immobilon®-P^{SQ} Transfer Membrane, Millipore). The membranes were fixed in 8% acetic acid after transferring the proteins in the case of BN-PAGE. Excess Coomassie Blue in the membranes was removed by incubating the membrane several minutes in methanol and then rinsing with water. Membranes were blocked using 5% skim milk in TBS buffer overnight. P13 (25) and BBA01 (27) antibodies were dissolved in 2.5% skim milk TBS buffer. For the secondary antibody an anti-rabbit antibody coupled to an alkaline phosphatase was used (anti-rabbit IgG alkaline phosphatase antibody produced in goat; Sigma). 5-bromo-4-chloro-3-indolyl phosphate/nitro blue tetrazolium (SIGMAFAST™ BCIP®/NBT, Sigma) was used to develop the membranes.

Mass Spectroscopy

For MALDI analysis a Proteomics analyzer 4700 (MALDI-TOF/TOF, Applied Biosystems, Darmstadt, Germany) was used. Matrix was α-Matrix (α-cyano-4-hydroxy-cinnamic acid) in overlay technique at 5 mg/ml in 50% acetonitrile, 0.1% TFA, 0.45-μl sample, and 0.45-μl matrix solution. The MALDI-MS and MS/MS measurements were performed with a 355-nm Nb-YAG laser in positive reflector mode with a 20-kV acceleration voltage.

Planar Lipid Bilayer

Two approaches were used in this study to characterize the pore-forming activity of the P13 porin; multichannel solvent-containing membranes (37) and single channel solvent-free membranes (38). The single channel conductance of P13 was studied using both methods, whereas ion selectivity, voltage-gating, and substrate specificity were studied using multichannel solvent-containing membranes.

[2] The abbreviations used are: nS, nanosiemens; BN-PAGE, blue native PAGE; Bis-Tris, 2-[bis(2-hydroxyethyl)amino]-2-(hydroxymethyl)propane-1,3-diol; Tricine, *N*-[2-hydroxy-1,1-bis(hydroxymethyl)ethyl]glycine; WB, Western blot; DPhPC, 1,2-diphytanoyl-*sn*-glycero-3-phosphocholine; DPhPG, 1,2-diphytanoyl-*sn*-glycero-3-phospho-1′-rac-glycerol; NE, nonelectrolyte.

Single Channel Conductance in Multichannel Solvent-containing Membranes—The planar lipid bilayer method has been described previously (39). The membranes were formed from a 1% (w/v) solution of DPhPC (1,2-diphytanoyl-*sn*-glycero-3-phosphocholine) or 1% DPhPG (1,2-diphytanoyl-*sn*-glycero-3-phospho-1′-rac-glycerol) (Avanti Polar Lipids, Alabaster, AL) in *n*-decane. The membranes had a surface of ~0.5 mm^2, and they were formed using a Teflon loop to spread the lipid over the aperture. The porin-containing protein fractions were 1:1 diluted in 1% Genapol (Roth) and added to the aqueous phase after the membrane had turned black. The membrane current was measured with a pair of reference Ag^+/AgCl electrodes with salt bridges switched in series with a voltage source and a highly sensitive current amplifier (Keithley 427). The signal was recorded by an analog strip chart recorder (Rikandenki). The temperature was kept at 20 °C throughout.

Single Channel Conductance at the Single Unit Level in Solvent-free Planar Lipid Bilayers—This approach has been described in detail previously (38, 40). Membranes were formed with DPhPC by employing the classic Montal and Mueller technique (38) were the solvent is depleted. Membranes had a surface of ~0.008 mm^2. Standard Ag^+/AgCl electrodes (World Precision Instruments) were placed in each chamber to measure the ion current. For single-channel measurements, small amounts of porin were added to the chamber. Spontaneous channel insertions were usually obtained applying 50-mV voltages. Conductance measurements were performed using an Axopatch 200B amplifier (Axon Instruments) in the voltage clamp mode. Signals were filtered by an on-board low pass Bessel filter at 600 Hz and recorded onto a computer hard drive with a sampling frequency of 2.5 kHz. The analysis of the conductance of the channels was performed using Clampfit (Axon Instruments) and Origin (Microcal Software Inc.).

Ion Selectivity—Zero-current membrane potential measurements were performed as described earlier (37). The membranes were formed in 0.1 M salt solution. A salt concentration gradient was gradually established across the membrane after porin insertions reached a stationary phase by the addition of 0.1 M salt solution to one side and 3 M salt solution to the other. Ions with a higher permeability through P13 cause charge separation across the membrane. As a result, a zero-current membrane potential is established when the electrochemical equilibrium is reached. Potentials were measured at the diluted side with a high impedance electrometer (Keithley 617) and analyzed using the Goldman-Hodgkin-Katz equation (37).

Voltage Gating—Voltage gating of the P13 porin was checked following the method described elsewhere (41) using membrane potentials in a range between −100 and +100 mV. The membrane conductance (G) as a function of voltage (V_m) was measured when the opening and closing of channels reached equilibrium after the membrane current decay due to the voltage step. The initial value of the conductance (G_o) obtained immediately after the onset of the voltage (which follows a linear function of the voltage) was divided by conductance (G) to analyze the gating of the channel.

Substrate Specificity—Blocking of P13 conductance by different substrates was investigated in the same way as the titration experiments to measure binding of maltooligosaccharides to carbohydrate-specific porins (15, 42). The measurements were performed with multi-channel membranes under stationary conditions obtained about 60–90 min after the addition of the protein to the planar lipid membranes. At that point, different solutes were added in defined concentrations to both sides of the membrane while stirring to allow equilibration. Specific transport of substances should create a block of the channel conductance due to an impaired ion flux through the channel caused by the binding of the solutes to the channel interior.

Channel Diameter Estimation Using Nonelectrolytes—The estimation of channel diameters using NEs is a method that has successfully been used previously (43). This method is based on the fact that small non-electrolytes that penetrate a channel will reduce its conductance due to an increase in the solution viscosity inside the channel. The conductance of the P13 channel was measured in 1 M KCl solutions each time containing a different NE (20% w/v) with increasing hydrodynamic radii (43–45). When the diameter of the NEs is increased, a point may be reached where bigger NEs cannot enter the channel, and its interior will be free of NEs. In these cases the conductance will be about the same as that measured in 1 M KCl solution free of nonelectrolytes. Following this protocol, the channel diameter should be approximately equal to the smallest NE that does not enter the channel and, therefore, does not reduce its conductance.

The size of a possible constriction inside the channel can be guessed using the channel filling concept. The filling of the channel (F) and its value in percentage (%F) were calculated as described elsewhere (43). The filling (F) is given by

$$F = [(G_o - G_i)/G_i]/[(X_o - X_i)/X_i] \quad \text{(Eq. 1)}$$

where G_o is the single-channel conductance in a solution without NE (1 M KCl), and G_i is the single-channel conductance in the presence of a solution containing 20% (w/v) of an NE. X_o and X_i correspond to the conductivity of the salt solution without NE and with 20% (w/v) of a defined NE, respectively. Assuming that the filling of the channel by two of the smallest NEs (in our study ethylene glycol and glycerol) is close to the maximum possible level, the filling can be calculated in terms of percentage (%F),

$$\%F = 2F_i/(F_1 + F_2)100\% \quad \text{(Eq. 2)}$$

where F_i is the filling in the presence of a given NE and F_1 and F_2 represent filling in the presence of ethylene glycol and glycerol in the bathing solution respectively. The radius of the constriction zone should be equal to the radius of the smallest NE that does not pass freely through the channel and, therefore, does not fill it by 100%.

The following NEs were used: ethylene glycol, glycerol, sorbitol, (all obtained from Sigma), polyethylene glycol (PEG) 200, PEG 300, PEG 400, PEG 600, and PEG 1,000 (all obtained from Fluka; Munich, Germany). Polyethylene glycols were the molecules of choice in our studies because in aqueous solutions they have a spherical shape (46, 47). At least 100 hundred P13 channels reconstituted into lipid membranes were analyzed to estimate the single channel conductance in the presence of the different NEs.

RESULTS

Composition of the Protein Complex—The B-fraction of *B. burgdorferi* was studied using BN-PAGE to identify possible formation of outer membrane complexes. Several protein complexes appeared on the BN-PAGE stained with silver nitrate. To further investigate if any of these complexes was related to P13, WBs were carried out using polyclonal antibodies against P13. A band with an apparent molecular mass of 300 kDa reacted strongly with the P13 antibody (Fig. 1*A*, *left*).

Faint traces of the P13 protein were also observed in Western blots of this first BN-PAGE especially in the low molecular mass range. To minimize this effect and increase the homogeneity of the sample, the P13 complex was extracted from the first BN-PAGE and reloaded again on a BN-PAGE of identical characteristics. The extraction of the P13 protein complex from the gel did not have any effect on its apparent molecular mass, which remained stable at 300 kDa. Western blots of the second BN-PAGE again confirmed the presence of P13 within the complex (Fig. 1*A*, *center*).

To study the protein complex in more detail, the band was also excised and extracted from the second BN-PAGE and resolved on a Tricine SDS-PAGE under denaturing conditions. A main band of 13 kDa was observed, which clearly reacted with the P13 antibody (Fig. 1*A*, *right*). Small amounts of other proteins were also observed in the gel when the staining procedure was prolonged.

Second dimension SDS-PAGE was also performed to differentiate between proteins smearing along the gel, which appear like lines crossing the gel horizontally, and well-defined components of the complex, which appear like small spots. Some proteins smeared along the first dimension and appeared in the second dimension as horizontal bands faintly stained. Those proteins were not considered as possible components of the complex. The gel also showed several spots apart from the one corresponding to the 13-kDa P13 protein with molecular masses of ~72 and 95 kDa (Fig. 1*B*, SDS-PAGE). When a gel of identical characteristics was used to perform a Western blot, the P13 antibody reacted with all these spots. Furthermore, other spots in the same vertical lane, which were not visible in the silver-stained gel, reacted also with the antibody (Fig. 1*B*, WB).

The outer membrane fraction of a *p13* knock-out mutant (*B. burgdorferi* P13–18; Ref. 32) was separated on a BN-PAGE in the same way as performed above for the wild type membrane fraction to confirm the role of P13 in the formation of the protein complex. The 300-kDa band was not visible after staining the gel with silver nitrate. The corresponding signal in the WB was also completely missing. That means not only that P13 was not expressed but also that the P13 antibody did not react with any other protein in the sample, for instance with the P13 paralogues (Fig. 2).

To study a possible role of the other proteins within the P13 paralogue protein family 48, especially the close-related protein BBA01, in the co-formation of the complex, an immunoblot against this paralogue was performed. However, BBA01 could not be detected in the 300-kDa complex eluted from a second BN-PAGE, which indicates that P13 forms the complex without requiring other P13 paralogues (results not shown). As discussed later, all other paralogues were absent in the sample tested.

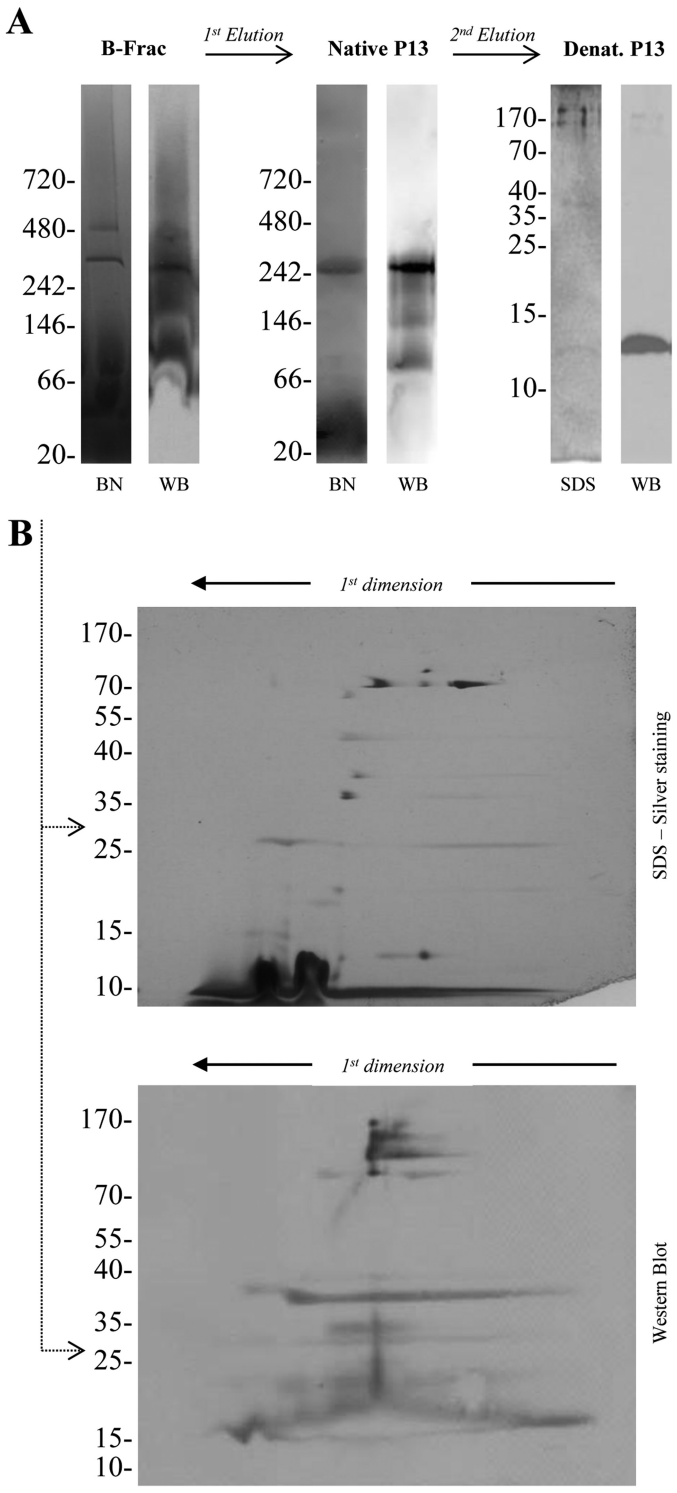

FIGURE 1. **BN- and SDS-PAGE analysis of the *B. burgdorferi* P13 complex.** *A*, the B-fraction-containing outer membrane proteins from *B. burgdorferi* B31 were separated on a BN-PAGE 4–16% acrylamide (Invitrogen), and P13 was detected by immunoblot (*left*). The band was excised from the gel and eluted with 0.1% digitonin, and the procedure was repeated in a second BN-PAGE/Western blot (*center*). The band was again excised and eluted and resolved on a Tricine SDS-PAGE plus Western blot (*right*). *B*, the first BN-PAGE containing the B-fraction of *B. burgdorferi* was also resolved in a second dimension SDS-PAGE with its correspondent P13 WB.

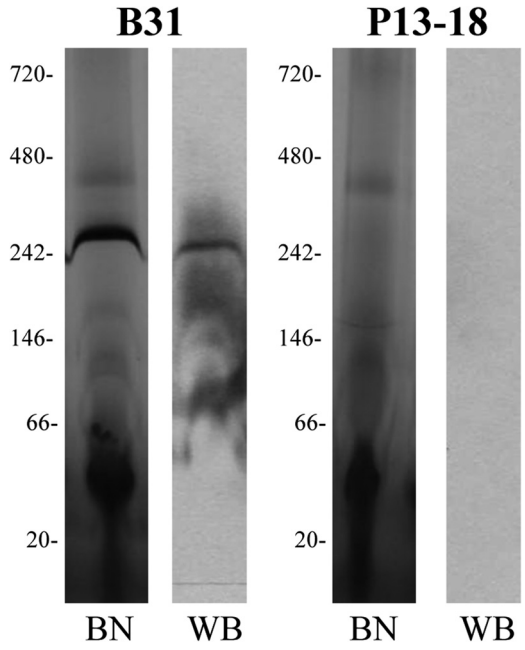

FIGURE 2. **Comparison of BN-PAGE and Western blot between *B. burgdorferi* wild type (*B31*) and a P13 knock out mutant (*P13–18*).** Approximately 0.8 μg of B-fraction from both strains was solubilized in digitonin and loaded in the BN-PAGE. The Western blots were performed using an antibody against P13.

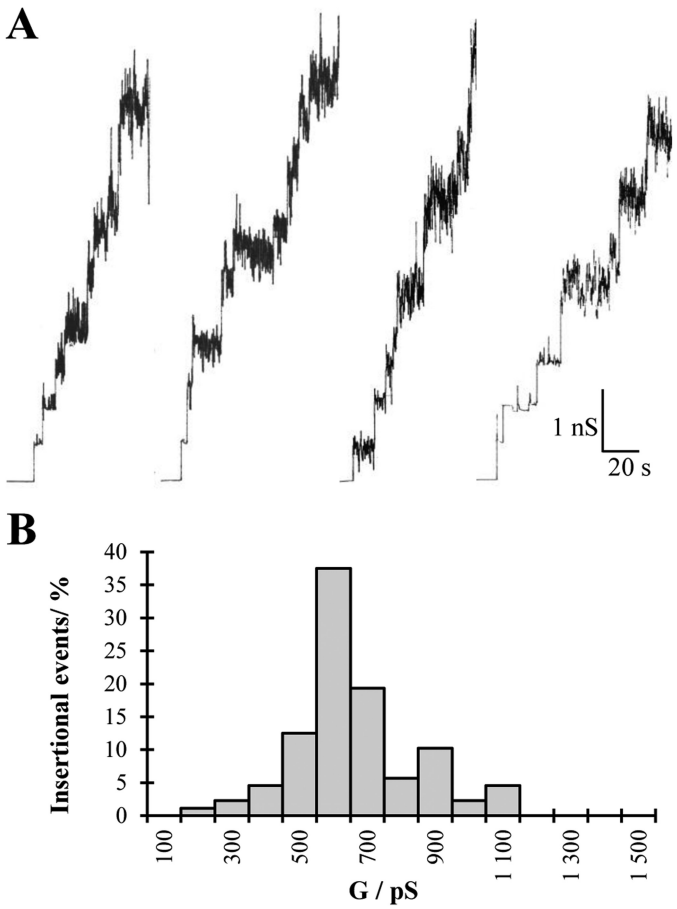

FIGURE 3. **Pore forming activity of *B. burgdorferi* P13 extracted from a secondary BN-PAGE.** Shown are four independent records of single channel insertions in a newly formed DPhPC membrane (1 M KCl, 20 mV) (*A*) and the corresponding histogram of the pore forming activity of the P13 protein complex using the planar lipid bilayer assay (*B*).

To further analyze the protein complex, it was subjected to mass spectrometry. Three samples were prepared for this analysis (supplemental Fig. S1). Sample 1 was obtained by excising the 300-kDa band from a second BN-PAGE, and samples 2 and 3 were obtained by cutting two pieces from a two-dimensional SDS-PAGE from a second BN-PAGE where the complex was resolved. Sample 2 covered several spots in an approximate horizontal range from 60 to 100 kDa, and sample 3 was a spot within an approximate range from 12–17 kDa. The proteins were trypsin-digested, and the masses obtained from the spectral data of these peptides (supplemental Figs. S2–S4) were compared with expected values computed from sequence database entries (NCBI, taxonomy bacterial proteins) according to the enzyme's cleavage specificity. The peptide identified with a higher intensity (>70%) in all three samples had a molecular mass of 1898.92 Da. This peptide was recognized as a P13 peptide with the sequence LTEIILPFTFANSYNR. In samples 1 and 2 a 1940.85-Da peptide was also observed with high intensity. This peptide was identified as a degradation product of pig trypsin, and it was not taken into consideration. In sample 2 other peptides with intensities between 40 and 70% were observed (masses 1306.50; 1492.70 and 1597.76 Da), but the search in the database did not report any significant matches for those peptides. The observation of the sequence of the BBA01 paralogue reported significant differences in trypsinization of this protein, and therefore, the peptide with a mass of 1898.92 is specific for P13 within the components of the paralogue family 48.

Single Channel Conductance—The P13 complex was run on two consecutive BN-PAGEs, and after the second elution the pore forming activity of this porin was studied. The addition of small amounts of the purified P13 complex (~10 ng/ml) to one or both sides of a planar lipid membrane made of phosphocholine/*n*-decane resulted after some delay in observation of step-like conductance increases with a value of 0.6 nS in 1 M KCl. Most of the steps were directed upward, indicating that the channels were in an open state under low voltage conditions (20 mV). The P13 channel had an intrinsic high noise that made it impossible after reconstitution of a few pores to identify the conductance of additional insertions (Fig. 3*A*). Therefore, only the first insertions in each membrane with clear conductance values were used to estimate the conductance of the P13 complex (Fig. 3*B*).

The pore-forming activity of the P13 complex was also measured in different KCl concentrations and in different electrolytes (LiCl and KCH_3COO) to gain some insight into the ion transport properties. The linear correlation between KCl concentration and the pore conductance is typical for general diffusion porins, which have no binding sites for anions or cations and where no net charges influence the pore conductance (Table 1). Comparison of measurements done in 1 M lithium chloride and in 1 M potassium acetate, where anions and cations differ inversely in hydrodynamic radius, with measurements done in 1 M KCl showed a similar decrease (0.2 and 0.25 nS, respectively) for the P13 single channel conductance. The comparable results obtained by exchanging the mobile ions K^+ and

TABLE 1

Single channel measurements of *B. burgdorferi* P13 in different KCl concentrations and different electrolytes

The P13 conductance (*G*) in each salt solution was taken from the highest conductance value observed in a Gaussian distribution of single channel conductance. To analyze P13 conductance, in each case at least 100 channels were reconstituted in DPhPC membranes at 20 mV voltage. The solutions were used unbuffered with a pH close to 6 unless otherwise indicated. The conductivity of each salt solution (χ) was measured at room temperature with a conductometer (Knick 703). The ion activities (γ) of the salts at 25 °C are given in parentheses (51).

Electrolyte	Concentration (γ)	χ	P13 *G*
	M	*mS/cm*	*nS*
KCl	0.1 (0.77)	13.1	0.05
	0.3 (0.68)	37.1	0.075
	1 (0.60)	106.5	0.6
	3 (0.56)	291.8	1.5
LiCl	1 (0.77)	70.3	0.2
KCH_3COO (pH 7)	1 (0.78)	68.6	0.25

Cl^- by the less mobile ions Li^+ and CH_3COO^- indicates that cations and anions have a similar permeability through the P13 complex, *i.e.* its selectivity is low if any (Table 1).

Two are the major lipids in the outer membrane of *B. burgdorferi*, phosphatidylcholine and phosphatidylglycerol. To study the possible influence of lipids, the P13 porin was as well measured in DPhPG membranes and 1 M KCl salt solution. P13 displayed in this type of membranes a very similar behavior to the one observed using DPhPC membranes. The sample was very active, and after several insertions the current noise hindered an accurate resolution of new insertions (Fig. 4*A*). Using the first insertions, a histogram was produced were the major conductance step was 0.6 nS in 1 M KCl (Fig. 4*B*).

Another reconstitution approach using solvent-free membranes was performed to study this porin at the single unit level. A single P13 channel was recorded with a high sampling digitizer (2.5 kHz) and a 600-Hz filter. Interestingly, the channel displayed some sub-states as well as short upwards spike-like fluctuations that shortly increased the conductance (Fig. 5*A*). These sub-states and fluctuations upward (Fig. 5*A*, conductance states 2 and 3, respectively) seem to be independent from the applied voltage as it is shown in the voltage-gating experiments (see below). A histogram summarizing the conductance data points revealed a predominant conductance of ~0.65 nS in 1 M KCl (Fig. 5*B*, conductance state 1). These results are somehow preliminary, and further analysis of this dynamic channel is required to clarify its several conductance states.

Ion Selectivity—Zero-current membrane potential measurements were also carried out to measure the ion selectivity of P13 in more detail. Membranes with >100 inserted P13 pores were used to perform these measurements. 5-Fold gradients of KCl, LiCl, and KCH_3COO were established across the membranes. Consequently, the zero-current potential for KCl was slightly negative (−3.4 mV) at the more diluted side of the membranes, which reflects some low anion selectivity. When LiCl was used, the diluted side was more negative (−11.9 mV), and when KCH_3COO was used, a positive potential was observed at the diluted side (17 mV). The ratios of the permeability P_{cation} and P_{anion} as calculated using the Goldman-Hodgkin-Katz equation were 0.8 for KCl, 0.40 for LiCl, and 3.5 for KCH_3COO, which means that the selectivity followed the mobility sequence of anions and cations in the aqueous phase, *i.e.* it is indeed water-filled (see Table 2). This supported the idea of a general diffusion channel with some minor selectivity for ions with a similar aqueous mobility.

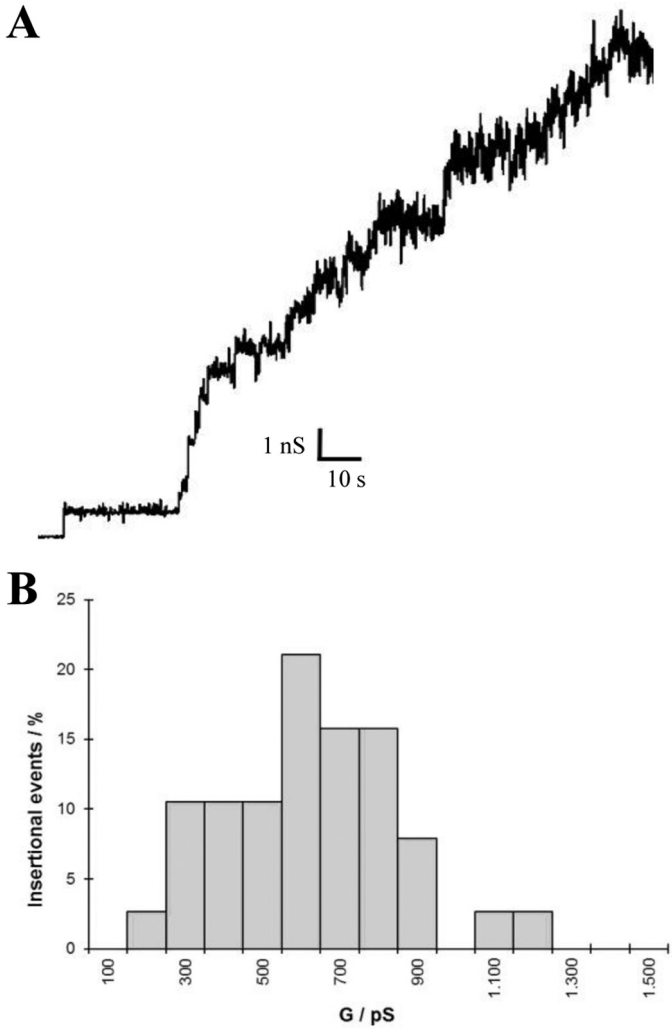

FIGURE 4. **Pore forming activity of *B. burgdorferi* P13 in DPhPG/*n*-decane membranes.** Shown are single channel recording of P13 extracted from a secondary BN-PAGE in 1 M KCl and 20 mV applied voltage (*A*) and the corresponding histogram of the pore forming activity of the P13 complex in DPhPG/*n*-decane membranes (*B*).

Voltage Gating—The effect of the voltage in the P13 pore was studied in a DPhPC membrane containing many P13 channels. Increasing positive and negative voltages were applied to study a possible gating of the pore. P13 showed a very low voltage-gating tendency between −100 and +100 mV (Fig. 6). For voltages up to ±40 mV the channel showed no decrease of the conductance at all. For higher voltages up to ±100 mV the P13 channel displayed minor gating, and the conductance values remained 85% or higher of its initial one.

Substrate Specificity—In these experiments we studied a possible substrate specificity of P13. In a first run we tested some physiologically important sugars such as glucose, fructose, galactose, ribose, maltose, lactose, and glucosamine. Similarly, we studied the effect of some amino acids such as glycine, cysteine, phenylalanine, histidine, arginine, or other molecules like ATP, ascorbic acid, or sodium phosphate on the conductance of P13. Interestingly, none of these molecules displayed any

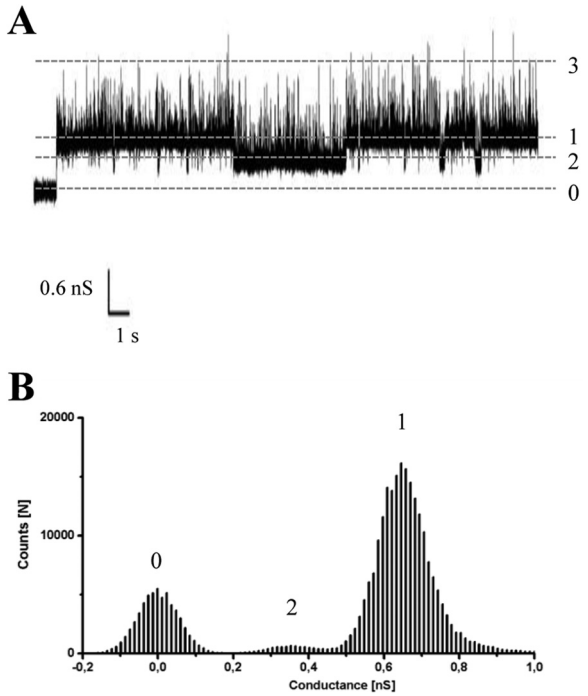

FIGURE 5. **Typical conductance through a single *B. burgdorferi* P13 channel (1 M KCl and 50 mV of applied voltage).** *A*, recording of a single P13 channel in a solvent-free DPhPC membrane. The different conductance states are indicated by the *dashed lines*. *B*, histogram summarizing its conductance from a 200-s measurement (400 μs sampling rate). The conductance state 3 is not appreciable in the histogram because the time in this conformation is very low in comparison with states 1 and 2. State 0 corresponds to the membrane with no pore inserted upon which a 50-mV voltage was already applied.

TABLE 2

Zero-current membrane potentials of PC/*n*-decane membranes in the presence of *B. burgdorferi* P13 measured for a 5-fold gradient of different salts (100 mM *versusp* 500 mM)

The zero-current membrane potentials V_m are defined as the difference between the potential at the dilute side and the potential at the concentrated side. The aqueous salt solutions were used unbuffered and had a pH of 6 if not indicated otherwise; T = 20 °C. The permeability ratio P_{cation}/P_{anion} was calculated using the Goldman-Hodgkin-Katz equation (37) from at least three individual experiments.

Salt	V_m	P_{cation}/P_{anion}
	mV	
KCl	−3.4	0.8
LiCl	−11.9	0.4
KCH_3COO (pH 7)	17.0	3.5

effect on the P13 channel conductance when added in a concentration range between 0.5 and 100 mM.

Channel Diameter—The estimation of a channel diameter using NEs is a method based on the fact that small non-electrolytes that penetrate a channel will reduce its conductance due to an increase in the viscosity of the solution in the channel interior that will modulate the ion flux (43). The conductance of the P13 channel was measured in a 1 M KCl solution supplemented with 20% (w/v) of different NEs with increasing hydrodynamic radii. Increasing the diameter of the NEs will lead to a point where the NEs will not be able to enter the channel and the channel interior will be free of NEs. In such a case the conductance of the P13 channel will be equal to the one measured in pure salt solution. By plotting the channel conductance as a function of the radii of the NEs, it is possible to correlate the hydrodynamic radius of the smallest NE that does not enter the

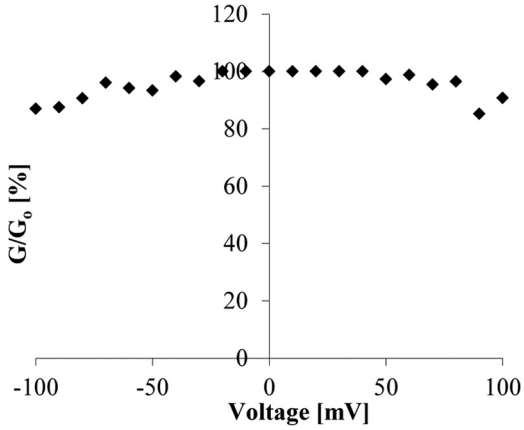

FIGURE 6. **Voltage-gating of *B. burgdorferi* P13.** Increasing positive and negative voltages were applied on a membrane saturated with P13 to study its gating. After applying the voltage and reaching equilibrium, the decrease in the membrane conductance (G_o/G) was calculated individually for each applied voltage. G_o = initial conductance right after applying voltage; G = conductance after reaching equilibrium.

pore with the diameter of the pore. The conductance of P13 as derived from the measurements with different NEs is summarized in Table 3. Molecular masses and hydrodynamic radii of the NEs and the specific aqueous conductivity of the solutions are also included in this table.

In the presence of ethylene glycol, glycerol, sorbitol, PEG 200, and PEG 300, the conductance of P13 was reduced to some extent (30–52% that of the original) (Fig. 7*A*). This decrease was correlated with the decrease of the specific conductivity of the salt solution in presence of the NEs. The P13 channel did not show any conductance reduction in the presence of PEG 400, PEG 600, and PEG 1,000 (Fig. 7*A*). This means that NEs with a hydrodynamic radius of 0.7 nm or larger were not able to enter the channel. In contrast to this, NEs with a hydrodynamic radius of 0.6 nm or smaller could enter the channel, which resulted in a conductance decrease. The results obtained suggested that the entrance of the P13 channel has approximately the size of PEG 400, *i.e.* its radius is estimated to be around 0.7 nm.

The channel-filling concept was also used here to analyze the idea of a possible constriction zone inside the channel. The radius of the constriction could be calculated using a previously proposed equation calculating the portion of the channel filled by each one of the NEs (43). This concept suggested that the radius of a constriction zone should be close to the radius of the smallest NE that does not fill the channel completely and, therefore, does not pass freely through the channel.

NEs such as ethylene glycol, glycerol, sorbitol, PEG 200, and PEG 300 showed an almost complete filling of the P13 channel, whereas PEG 400 and bigger had filling values close to 0 (Table 3 and Fig. 7*B*). NEs that filled the channel only partially could not be identified among the different NEs, which means that the channel has no obvious constriction, *i.e.* looks more like a cylinder. The channel filling with sorbitol and PEG 300 was somewhat >100%. To test if that effect was due to a special interaction of the sorbitol or PEG 300 with the channel interior, we performed titration experiments of multichannel membranes with these molecules in the millimolar range as previ-

TABLE 3

Average single channel conductance of *B. burgdorferi* P13 in the presence of different NEs in the bath solution

Average single channel conductances (*G*) and their S.D. (G ± S.D.) were calculated from at least 100 conductance steps. The aqueous phase contained 1 M KCl and the corresponding nonelectrolyte at a concentration of 20% (w/v). V_m = 20 mV; T = 20 °C; Mr = molecular mass; *r* = hydrodynamic radius (M_r and *r* of the nonelectrolytes were taken from previous publications (43–45)); χ is the conductivity of the aqueous solutions. Channel filling (*F*) and percentage of channel filling (%*F*) were calculated as described elsewhere (43). Et.Gl, ethylene glycol.

				P13			
NEs	Mr	*r*	χ	*G* ± S.D.	%*G*	*F*	%*F*
	g/mol	*nm*	*mS cm*$^{-1}$	*nS*			
None			110.30	0.6 ± 0.18	100		
Et.Gl	62	0.26	57.20	0.3 ± 0.09	50	1.08	114.63
Glycerol	92	0.31	49.10	0.3 ± 0.07	50	0.80	85.37
Sorbitol	182	0.39	57.80	0.2 ± 0.07	33	2.20	234.31
PEG 200	200	0.50	46.10	0.3 ± 0.09	50	0.72	76.40
PEG 300	300	0.60	45.50	0.2 ± 0.07	33	1.40	149.44
PEG 400	400	0.70	46.40	0.6 ± 0.07	100	0.00	0.00
PEG 600	600	0.80	54.10	0.6 ± 0.11	100	0.00	0.00
PEG 1000	1000	0.94	49.50	0.65 ± 0.09	108	−0.06	−6.66

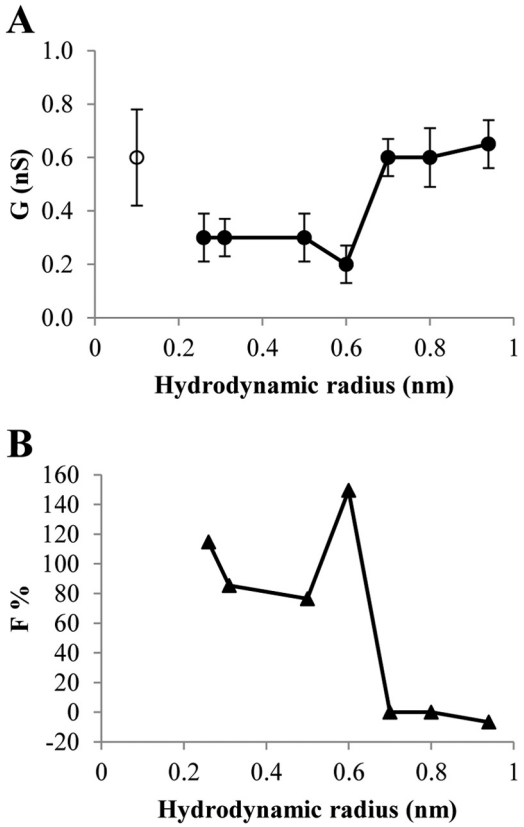

FIGURE 7. ***B. burgdorferi* P13 conductance and channel filling in presence of different non-electrolytes.** *A*, the conductance of P13 (*G*) was measured in 1 M KCl (*open circles*) and 1 M KCl containing 20% (v/w) of an NE (*filled circles*). *B*, the channel filling in percentage (%*F*) was calculated using the formula described elsewhere (43). The conductance and channel filling corresponding to sorbitol were not included in these diagrams due to its unreasonable values, which could indicate a possible interaction of this compound with the channel interior.

ously described in the substrate specificity section. In these experiments we could not detect any effect of PEG 300 or sorbitol on the P13 conductance.

A possible orientation of the P13 channel in planar bilayers was studied using different approaches. First, P13 was added only to one side of the membrane, and different positive and negative voltages were applied. P13 displayed a very similar gating behavior when applying positive or negative voltages. These results were as well very similar to those obtained when P13 was added to both sides (Fig. 4), preventing any conclusion. In a second approach a possible orientation of P13 was studied while decreasing the pH. The pH was decreased only in one side of the membrane, whereas the other side remained around pH 6. As described previously for LamB (48), this decrease can cause a gating of the pores probably because the charged loops bend over the channel blocking its conductance. If the channel is oriented, the blockage of the channel will only occur when the pH is decreased in one of the sides. Unfortunately, the results decreasing the pH were not consistent, and neither approach led to a clear identification of an oriented insertion of the P13 channel into DPhPC membranes.

DISCUSSION

Structure of the P13 Pore-forming Complex—P13 isolated from the outer membrane of *B. burgdorferi* has been described as a protein with porin properties, although its structure differs considerably from those of typical Gram-negative bacterial porins (49).

We used BN-PAGE/WB to study the P13 protein complex in detail. Western blots demonstrated the presence of P13 in a 300-kDa band on the gels. Globular or elongated complexes may run with different speed in BN-PAGE. This issue is addressed in detail in a previous study, where a maximal molecular mass deviation of 15% was estimated for different kinds of proteins (50). This estimation seems to be valid as long as the proteins either bind Coomassie or have isoelectric points (pI) below or equal to 8.6 (50). According to this study, proteins with higher pI values, like P13, which binds Coomassie but has a pI close to 9.5, could show a molecular mass up to 30% higher than the real molecular mass (50). How much higher is difficult to predict. The apparent molecular mass of the P13 complex was ~300 kDa on BN-PAGE. If it is assumed that this could be at maximum 30% too high, the molecular mass of the complex could still be around 200 kDa. This estimation is supported by the Western blots of the two-dimensional gel where some P13 spots, probably complexes retaining the native conformation in the SDS-PAGE, appeared to have a molecular mass close to 200 kDa (Fig. 1*B*).

SDS-PAGE of the P13 complex in the second dimension was also used to study if other proteins were part of the protein complex (Fig. 1*B*). A clear spot of ~13 kDa was observed when the gel was stained with silver nitrate. Two additional spots

were usually observed on the gel with molecular masses around 72 and 95 kDa. The corresponding Western blots demonstrated that these three spots contained also P13. Additional protein spots in the upper molecular mass range reacted also with the P13 antibody (Fig. 1*B*, WB). Based on that, the P13 complex appeared to be resistant, at least partially, to denaturing agents like SDS or DTT. The different spots in the same vertical lane could, therefore, be different dissociation states of P13 from the P13 complex. A cross-reaction with other proteins was unlikely because antibodies against P13 did not interact with other proteins in the *p13*-deficient mutant.

It is noteworthy that the resolution of the P13 complex in two-dimensional SDS-PAGE and in Tricine SDS-PAGE after elution and heating of the sample showed that the P13 complex is a homo-oligomer. This fact is also supported by the MS analysis of the protein complex.

In the *B. burgdorferi* B31 genome eight paralogues have been found for the p13 gene (bb0034), constituting the gene family 48. Two are pseudogenes (bbj02.1 and bbq81), one has an authentic frameshift producing a completely different peptide (bbg03), and another is located inside bbj02.1 (bbj03). The remaining four (BBA01, BBI31, BBH41, and BBQ06) show a higher similarity to P13 (25), and therefore, they may share a similar function. A previous study showed that in high passage *B. burgdorferi* B31 cultures the plasmids containing some of these paralogues are lost, and only BBA01 was still present (27). The high passage strain and an immunoblot against BBA01 contradict a possible presence of these polypeptides within the 300-kDa complex. Whether these paralogues form similar protein complexes as P13 or not is an open question, and further studies need to be done to clarify this issue in more detail.

Pore-forming Activity of the P13 Complex—The pore-forming activity of the P13 complex was measured in lipid bilayer experiments after gel elution. The conductance of the pore formed by P13 was estimated in previous studies to be 3.5 nS in 1 M KCl (24, 28). However, none of the samples isolated in this study from different BN-PAGEs showed such a pore-forming activity. The planar lipid bilayer measurements of the 300-kDa band and the realization of the corresponding histogram revealed a pore-forming activity of about 0.6 nS in 1 M KCl. This result is in some contradiction to the previous pore forming activity observed for P13 (24, 28). The pores obtained from the eluted 300-kDa band showed some intrinsic noise, and after reconstitution of some channels it was difficult to evaluate the exact conductance of new insertions (see Fig. 3*A*). Although the noise was very high from that point on, the membrane conductance increased constantly. To check the integrity of the eluted P13 complex, the protein was loaded on a second and even a third BN-PAGE that displayed the same molecular mass and, therefore, retained its native state. It is noteworthy that the P66 complex previously eluted from BN-PAGE also retained its pore-forming activity after elution from BN-PAGE (52).

A similar 0.6-nS pore-forming activity as the one found here was previously described together with 12.6-nS pores in outer membrane vesicles from *B. burgdorferi* B31 (53). This 0.6-nS pore-forming activity was afterward attributed to Oms28 (29). However, in another study the role of Oms28 as a porin was questioned because of its apparent location in the periplasmic space (30). The existence of a channel-forming protein in the outer membrane of *Borrelia* with a conductance of 0.6 nS in 1 M KCl has been observed several times in our laboratory when B-fractions were analyzed. The 300-kDa complex isolated from BN-PAGE containing P13 has the same conductance and can, therefore, be considered as the complex responsible for such a pore-forming activity.

Previous studies of the B-fraction from a *p66* knock-out mutant and a *p13/p66* double knock-out could support this assumption (32). The B-fraction of the *p66* knock-out mutant did not show any 3.5-nS activity at all, and the double *p13/p66* knock-out reduced the conductance of the porins in the sample to 300 pS or below, where the 0.6-nS activity was also missing (32).

The kind of lipid used to form the membrane and the presence of solvents in it did not seem to influence the conductance of the P13 channel as demonstrated in the experiments of Figs. 4 and 5. Two phospholipids constitute the outer membrane of *Borrelia*, phosphatidylcholine, and phosphatidylglycerol (54). Side chain variants of these lipids, diphytanoyl phosphatidylcholine and diphytanoyl phosphatidylglycerol, were used to perform planar lipid membrane experiments. Phospholipids containing diphytanoyl fatty acid side chains are commonly used to form stable artificial lipid membranes within a wide temperature range without a phase transition (from −120 to +80 °C for DPhPC) (55). The channel displayed the same 0.6-nS conductance independently of the lipid used. In reference to the presence of solvents in the membrane the study of single P13 units in solvent-free membranes showed a very similar channel conductance of 0.65 nS. Furthermore, the study of a single P13 unit in solvent-free membranes allowed the observation of a high intrinsic noise of this channel. This noise differed to some extend from channel to channel.

Size of the Pore Formed by the P13 Complex—We used different NEs to determine the channel diameter of the P13 pore employing a previously suggested method (43, 45, 56). Because NEs are uncharged molecules, they avoid attraction/repulsion forces between ions and charges in the channel interior. In addition, the determination of the channel diameter using NEs is not influenced by the conformation of the pores when they represent oligomeric channels in particular trimers such as many porins in Gram-negative bacteria. From the experiments with NEs we calculated a diameter of about 1.4 nm for the P13 complex. These calculations include an estimated error of ±0.1 nm caused by a certain smearing of the molecular masses of the individual NEs influencing their hydrodynamic radii (45, 56). According to our results, a constriction inside the P13 channel cannot be excluded completely, but this is rather unlikely because the constriction has a similar diameter as the channel opening as judged from the results of estimating the channel filling.

Small molecules up to 400 g/mol seem to have access to the channel interior and, therefore, could diffuse in the periplasmic space of *B. burgdorferi* through P13. It is well known that porins in Gram-negative bacteria represent a pathway for antibiotics to cross the outer membrane (57–59). Several antibiotics used in the treatment against *Borrelia* (60) such as amoxicillin (365 g/mol) are under the molecular weight cut-off described in this

paper for possible P13 substrates. Therefore, this channel could play a role in the translocation and action of antibiotics used to treat infections by *Borrelia*.

In this study we investigated structure and composition of the P13 complex from *B. burgdorferi* outer membrane. The results suggested that P13 forms a complex with a molecular mass of about 200 to 300 kDa. P13 is the only polypeptide that is present in the complex. The P13 complex is a homo-oligomer, and it is composed of a high number of P13 monomers, although further studies need to be done to assign the number of monomers and pores in the complex. Similarly we studied the pore-forming activity of the P13 complex in detail and could attribute it to a single channel conductance of 0.6 nS in 1 M KCl. The channel has minor selectivity for ions, is voltage-gating-independent up to ± 100 mV, and seems to be a general diffusion channel. The molecular mass cut-off of the P13 complex was estimated to be around 400 g/mol from experiments with NEs meaning the channel diameter is around 1.4 (±0.1) nm.

REFERENCES

1. Woese, C. R. (1987) Bacterial evolution. *Microbiol. Rev.* **51,** 221–271
2. Obermeier, O. H. F., and Zeiss, H. (1873) *Die entdeckung von fadenförmigen gebilden im blut von rückfallfieberkranken (1873) Eingeleitet und herausgegeben von Dr. Heinz Zeiss*, Leipzig, J. A. Barth, 1926
3. Burgdorfer, W. (1984) Discovery of the Lyme disease spirochete and its relation to tick vectors. *Yale J. Biol. Med.* **57,** 515–520
4. Burgdorfer, W., Barbour, A. G., Hayes, S. F., Benach, J. L., Grunwaldt, E., and Davis, J. P. (1982) Lyme disease-a tick-borne spirochetosis? *Science* **216,** 1317–1319
5. Steere, A. C. (2001) Lyme disease. *N. Engl. J. Med.* **345,** 115–125
6. Steere, A. C. (2006) Lyme borreliosis in 2005, 30 years after initial observations in Lyme Connecticut. *Wien. Klin. Wochenschr.* **118,** 625–633
7. Barbour, A. G., and Hayes, S. F. (1986) Biology of *Borrelia* species. *Microbiol. Rev.* **50,** 381–400
8. Fraser, C. M., Casjens, S., Huang, W. M., Sutton, G. G., Clayton, R., Lathigra, R., White, O., Ketchum, K. A., Dodson, R., Hickey, E. K., Gwinn, M., Dougherty, B., Tomb, J. F., Fleischmann, R. D., Richardson, D., Peterson, J., Kerlavage, A. R., Quackenbush, J., Salzberg, S., Hanson, M., van Vugt, R., Palmer, N., Adams, M. D., Gocayne, J., Weidman, J., Utterback, T., Watthey, L., McDonald, L., Artiach, P., Bowman, C., Garland, S., Fuji, C., Cotton, M. D., Horst, K., Roberts, K., Hatch, B., Smith, H. O., and Venter, J. C. (1997) Genomic sequence of a Lyme disease spirochaete, *Borrelia burgdorferi*. *Nature* **390,** 580–586
9. Hasle, G. (2013) Transport of ixodid ticks and tick-borne pathogens by migratory birds. *Front Cell Infect. Microbiol.* **3,** 48
10. Mannelli, A., Bertolotti, L., Gern, L., and Gray, J. (2012) Ecology of *Borrelia burgdorferi* sensu lato in Europe: transmission dynamics in multi-host systems, influence of molecular processes and effects of climate change. *FEMS Microbiol. Rev.* **36,** 837–861
11. Benz, R. (1994) Solute uptake through bacterial outer membranes. in *Bacterial Cell Wall* (Ghuysen, J. M., and Hakenbeck, R., eds.) pp. 397–423, Elsevier Science Publishing Co., Inc., New York
12. Achouak, W., Heulin, T., and Pagès, J. M. (2001) Multiple facets of bacterial porins. *FEMS Microbiol. Lett.* **199,** 1–7
13. Maier, C., Bremer, E., Schmid, A., and Benz, R. (1988) Pore-forming activity of the Tsx protein from the outer membrane of *Escherichia coli*. Demonstration of a nucleoside-specific binding site. *J. Biol. Chem.* **263,** 2493–2499
14. Benz, R., Schmid, A., Maier, C., and Bremer, E. (1988) Characterization of the nucleoside-binding site inside the Tsx channel of *Escherichia coli* outer membrane. Reconstitution experiments with lipid bilayer membranes. *Eur. J. Biochem.* **176,** 699–705
15. Benz, R., Schmid, A., and Vos-Scheperkeuter, G. H. (1987) Mechanism of sugar transport through the sugar-specific LamB channel of *Escherichia coli* outer membrane. *J. Membr. Biol.* **100,** 21–29
16. Hancock, R. E., and Benz, R. (1986) Demonstration and chemical modification of a specific phosphate binding site in the phosphate-starvation-inducible outer membrane porin protein P of *Pseudomonas aeruginosa*. *Biochim. Biophys. Acta* **860,** 699–707
17. Kim, B. H., Andersen, C., and Benz, R. (2001) Identification of a cell wall channel of *Streptomyces griseus*: the channel contains a binding site for streptomycin. *Mol. Microbiol.* **41,** 665–673
18. Bárcena-Uribarri, I., Thein, M., Sacher, A., Bunikis, I., Bonde, M., Bergström, S., and Benz, R. (2010) P66 porins are present in both Lyme disease and relapsing fever spirochetes: a comparison of the biophysical properties of P66 porins from six *Borrelia* species. *Biochim. Biophys. Acta* **1798,** 1197–1203
19. Skare, J. T., Mirzabekov, T. A., Shang, E. S., Blanco, D. R., Erdjument-Bromage, H., Bunikis, J., Bergström, S., Tempst, P., Kagan, B. L., Miller, J. N., and Lovett, M. A. (1997) The Oms66 (p66) protein is a *Borrelia burgdorferi* porin. *Infect. Immun.* **65,** 3654–3661
20. Coburn, J., Chege, W., Magoun, L., Bodary, S. C., and Leong, J. M. (1999) Characterization of a candidate *Borrelia burgdorferi* β3-chain integrin ligand identified using a phage display library. *Mol. Microbiol.* **34,** 926–940
21. Coburn, J., and Cugini, C. (2003) Targeted mutation of the outer membrane protein P66 disrupts attachment of the Lyme disease agent, *Borrelia burgdorferi*, to integrin αvβ3. *Proc. Natl. Acad. Sci. U.S.A.* **100,** 7301–7306
22. Thein, M., Bunikis, I., Denker, K., Larsson, C., Cutler, S., Drancourt, M., Schwan, T. G., Mentele, R., Lottspeich, F., Bergström, S., and Benz, R. (2008) Oms38 is the first identified pore-forming protein in the outer membrane of relapsing fever spirochetes. *J. Bacteriol.* **190,** 7035–7042
23. Thein, M., Bonde, M., Bunikis, I., Denker, K., Sickmann, A., Bergström, S., and Benz, R. (2012) DipA, a pore-forming protein in the outer membrane of Lyme disease spirochetes exhibits specificity for the permeation of dicarboxylates. *PLoS ONE* **7,** e36523
24. Ostberg, Y., Pinne, M., Benz, R., Rosa, P., and Bergström, S. (2002) Elimination of channel-forming activity by insertional inactivation of the *p13* gene in *Borrelia burgdorferi*. *J. Bacteriol.* **184,** 6811–6819
25. Noppa, L., Ostberg, Y., Lavrinovicha, M., and Bergström, S. (2001) P13, an integral membrane protein of *Borrelia burgdorferi*, is C-terminally processed and contains surface-exposed domains. *Infect. Immun.* **69,** 3323–3334
26. Kumru, O. S., Bunikis, I., Sorokina, I., Bergström, S., and Zückert, W. R. (2011) Specificity and role of the *Borrelia burgdorferi* CtpA protease in outer membrane protein processing. *J. Bacteriol.* **193,** 5759–5765
27. Pinne, M., Ostberg, Y., Comstedt, P., and Bergström, S. (2004) Molecular analysis of the channel-forming protein P13 and its paralogue family 48 from different Lyme disease *Borrelia* species. *Microbiology* **150,** 549–559
28. Pinne, M., Denker, K., Nilsson, E., Benz, R., and Bergström, S. (2006) The BBA01 protein, a member of paralog family 48 from *Borrelia burgdorferi*, is potentially interchangeable with the channel-forming protein P13. *J. Bacteriol.* **188,** 4207–4217
29. Skare, J. T., Champion, C. I., Mirzabekov, T. A., Shang, E. S., Blanco, D. R., Erdjument-Bromage, H., Tempst, P., Kagan, B. L., Miller, J. N., and Lovett, M. A. (1996) Porin activity of the native and recombinant outer membrane protein Oms28 of *Borrelia burgdorferi*. *J. Bacteriol.* **178,** 4909–4918
30. Mulay, V., Caimano, M. J., Liveris, D., Desrosiers, D. C., Radolf, J. D., and Schwartz, I. (2007) *Borrelia burgdorferi* BBA74, a periplasmic protein associated with the outer membrane, lacks porin-like properties. *J. Bacteriol.* **189,** 2063–2068
31. Cluss, R. G., Silverman, D. A., and Stafford, T. R. (2004) Extracellular secretion of the *Borrelia burgdorferi* Oms28 porin and Bgp, a glycosaminoglycan binding protein. *Infect. Immun.* **72,** 6279–6286
32. Pinne, M., Thein, M., Denker, K., Benz, R., Coburn, J., and Bergström, S. (2007) Elimination of channel-forming activity by insertional inactivation of the p66 gene in *Borrelia burgdorferi*. *FEMS Microbiol. Lett.* **266,** 241–249
33. Barbour, A. G. (1984) Isolation and cultivation of Lyme disease spirochetes. *Yale. J. Biol. Med.* **57,** 521–525
34. Magnarelli, L. A., Anderson, J. F., and Barbour, A. G. (1989) Enzyme-linked immunosorbent assays for Lyme disease: reactivity of subunits of *Borrelia burgdorferi*. *J. Infect. Dis.* **159,** 43–49

35. Schägger, H. (2006) Tricine-SDS-PAGE. *Nat. Protoc.* **1,** 16–22
36. Blum, H., Beier, H., and Gross, H. J. (1987) Improved silver staining of plant proteins, RNA and DNA in polyacrylamide gels. *Electrophoresis* **8,** 93–99
37. Benz, R., Janko, K., and Läuger, P. (1979) Ionic selectivity of pores formed by the matrix protein (porin) of *Escherichia coli*. *Biochim. Biophys. Acta* **551,** 238–247
38. Montal, M., and Mueller, P. (1972) Formation of bimolecular membranes from lipid monolayers and a study of their electrical properties. *Proc. Natl. Acad. Sci. U.S.A.* **69,** 3561–3566
39. Benz, R., Janko, K., Boos, W., and Läuger, P. (1978) Formation of large, ion-permeable membrane channels by the matrix protein (porin) of *Escherichia coli*. *Biochim. Biophys. Acta* **511,** 305–319
40. Mahendran, K. R., Hajjar, E., Mach, T., Lovelle, M., Kumar, A., Sousa, I., Spiga, E., Weingart, H., Gameiro, P., Winterhalter, M., and Ceccarelli, M. (2010) Molecular basis of enrofloxacin translocation through OmpF, an outer membrane channel of *Escherichia coli*: when binding does not imply translocation. *J. Phys. Chem. B* **114,** 5170–5179
41. Ludwig, O., De Pinto, V., Palmieri, F., and Benz, R. (1986) Pore formation by the mitochondrial porin of rat brain in lipid bilayer membranes. *Biochim. Biophys. Acta* **860,** 268–276
42. Benz, R., Schmid, A., Nakae, T., and Vos-Scheperkeuter, G. H. (1986) Pore formation by LamB of *Escherichia coli* in lipid bilayer membranes. *J. Bacteriol.* **165,** 978–986
43. Krasilnikov, O. V., Da Cruz, J. B., Yuldasheva, L. N., Varanda, W. A., and Nogueira, R. A. (1998) A novel approach to study the geometry of the water lumen of ion channels: colicin Ia channels in planar lipid bilayers. *J. Membr. Biol.* **161,** 83–92
44. Sabirov, R. Z., Krasilnikov, O. V., Ternovsky, V. I., and Merzliak, P. G. (1993) Relation between ionic channel conductance and conductivity of media containing different nonelectrolytes. A novel method of pore size determination. *Gen. Physiol. Biophys.* **12,** 95–111
45. Krasilnikov, O. V., Sabirov, R. Z., Ternovsky, V. I., Merzliak, P. G., and Muratkhodjaev, J. N. (1992) A simple method for the determination of the pore radius of ion channels in planar lipid bilayer membranes. *FEMS Microbiol. Immunol.* **5,** 93–100
46. Mark, J. E., and Flory, P. J. (1965) The configuration of the polyoxyethylene chain. *J. Am. Chem. Soc.* **87,** 1415–1422
47. Rempp, P. (1957) Contribution a l'étude des solution de molecules en chain a squelette oxigène. *J. Chem. Phys.* **54,** 432–453
48. Andersen, C., Schiffler, B., Charbit, A., and Benz, R. (2002) PH-induced collapse of the extracellular loops closes *Escherichia coli* maltoporin and allows the study of asymmetric sugar binding. *J. Biol. Chem.* **277,** 41318–41325
49. Benz, R. (ed) (2001) *Porins: Structure and Function*, WILEY-VCH Verlag GmbH, Weinheim, Germany
50. Schägger, H., Cramer, W. A., and von Jagow, G. (1994) Analysis of molecular masses and oligomeric states of protein complexes by blue native electrophoresis and isolation of membrane protein complexes by two-dimensional native electrophoresis. *Anal. Biochem.* **217,** 220–230
51. Lide, D. R. (ed) (1998) *CRC Handbook of Chemistry and Physics*, 71st Edition, Section 5, p. 99, CRC Press, Inc., Boca Raton, FL
52. Bárcena-Uribarri, I., Thein, M., Maier, E., Bonde, M., Bergström, S., and Benz, R. (2013) Use of nonelectrolytes reveals the channel size and oligomeric constitution of the *Borrelia burgdorferi* P66 porin. *PLoS ONE* **8,** e78272
53. Skare, J. T., Shang, E. S., Foley, D. M., Blanco, D. R., Champion, C. I., Mirzabekov, T., Sokolov, Y., Kagan, B. L., Miller, J. N., and Lovett, M. A. (1995) Virulent strain associated outer membrane proteins of *Borrelia burgdorferi*. *J. Clin. Invest.* **96,** 2380–2392
54. Belisle, J. T., Brandt, M. E., Radolf, J. D., and Norgard, M. V. (1994) Fatty acids of *Treponema pallidum* and *Borrelia burgdorferi* lipoproteins. *J. Bacteriol.* **176,** 2151–2157
55. Tristram-Nagle, S., Kim, D. J., Akhunzada, N., Kucerka, N., Mathai, J. C., Katsaras, J., Zeidel, M., and Nagle, J. F. (2010) Structure and water permeability of fully hydrated diphytanoylPC. *Chem. Phys. Lipids* **163,** 630–637
56. Nablo, B. J., Halverson, K. M., Robertson, J. W., Nguyen, T. L., Panchal, R. G., Gussio, R., Bavari, S., Krasilnikov, O. V., and Kasianowicz, J. J. (2008) Sizing the *Bacillus anthracis* PA63 channel with nonelectrolyte poly(ethylene glycols). *Biophys. J.* **95,** 1157–1164
57. Nikaido, H. (2003) Molecular basis of bacterial outer membrane permeability revisited. *Microbiol. Mol. Biol. Rev.* **67,** 593–656
58. Hancock, R. E., and Bell, A. (1988) Antibiotic uptake into gram-negative bacteria. *Eur. J. Clin. Microbiol. Infect. Dis.* **7,** 713–720
59. Delcour, A. H. (2009) Outer membrane permeability and antibiotic resistance. *Biochim. Biophys. Acta* **1794,** 808–816
60. Sicklinger, M., Wienecke, R., and Neubert, U. (2003) *In vitro* susceptibility testing of four antibiotics against *Borrelia burgdorferi*: a comparison of results for the three genospecies *Borrelia afzelii*, *Borrelia garinii*, and *Borrelia burgdorferi* sensu stricto. *J. Clin. Microbiol.* **41,** 1791–1793